"Sokol" high-power 24-channel facility for spherical irradiation of targets

I. A. Abramov, V. V. Volenko, N. P. Voloshin, A. I. Zuev, Yu. A. Zysin, A. F. Ivanov, Yu. M. Kononenko, F. P. Krupin, V. A. Lykov, L. A. Myalitsin, L. A. Osadchuk, I. A. Pekhterev, and A. I. Saukov

The "Sokol" 24-channel neodymium-glass laser facility for spherical irradiation of targets is described. A laser pulse energy $E_L = 300$ J at a peak power $P \sim 0.4$ TW and beam divergence $2\alpha \approx 3 \times 10^{-4}$ rad are attained. The target-irradiation system has a 12-beam geometry and the achieved irradiance uniformity is $\gamma \approx 10$–20% at an irradiation efficiency $\eta \approx 50$–70%. In the first stage of the experiments, the efficiency of laser-energy absorption is investigated and the energy absorbed is determined by the "shock-wave" technique. A gasdynamic program that takes into account the features peculiar to laser heating of targets is developed and leads to good agreement between the experimental and calculated $(R–t)$ parameters of the shock wave. An analytic expression is obtained to interpolate the gasdynamic calculation results with accuracy ~ 1% for absorbed energies from 5 to 50 J and for a residual gas pressure 3–5 Torr.

PACS numbers: 52.50.Jm

INTRODUCTION

Progress in controlled thermonuclear fusion in the last few years is characterized by an ever increasing interest in laser-driven thermonuclear fusion (LTF). The reason is that lasers are capable of producing a high energy density within times comparable with the time of the hydrodynamic expansion of the target. The first possibility of such a use of lasers was discussed by Basov and Krokhin.[1,2] Estimates and calculations presented in subsequent papers devoted to LTF have shown that the most promising is a regime with an appreciable compression of the thermonuclear fueld. The laser energy E_L required to realize a thermonuclear flash depends on the degree δ of fuel compression like $E_L \propto \delta^{-2}$ (Ref. 3). It is shown in Refs. 4–7 that under sufficiently realistic assumptions with respect to the required laser-pulse parameters and the target construction, the laser energy needed to reach a thermonuclear flash is ~ 100 kJ.

The construction of laser facilities of scale sufficient to satisfy the conditions for a thermonuclear flash, and all the more to reach the appreciable gain needed to produce an energywise profitable reactor, is still a matter of the future. Nevertheless, experimental study of important aspects of the physical processes typical of LTF, for the purpose of verifying critically the important predictions of the theory, is possible by using model laser facilities of much smaller scale. The fact that the technology of neodymium-class lasers has recently outstripped that of lasers of other types has caused the LTF model facilities in most countries to be based precisely on such lasers.

Model facilities for spherical irradiation of targets in the USSR and US differ in many characteristics, involving both the approach to the performance of the experiments on LTF at a given stage and the principles of constructing such facilities.

For the experiments carried out with the model facilities in the US (the KMS-Fusion laser facility; the Janus, Cyclops, Argus, and the later-generation Shiva facilities developed within the framework of a single program at the Livermore Laboratory) the targets are irradiated by pulses of duration $\sim 10^{-6}$ sec at target irradiances 10^{15}–10^{17} W/cm^2 (Refs. 8–11). On the other hand, experiments with the facilities in operation in the USSR, namely "Kal'mar"[12-13] and "Sokol," which make up together with the next-generation "Del'fin" facility being developed at the Physics Institute of the USSR Academy of Sciences,[14] listed in increasing order of energy, use longer durations ($\sim 10^{-9}$ sec) pulses to irradiate the target and more moderate densities of the optical radiation flux at the target, 10^{13}–10^{15} W/cm^2.

A characteristic feature of the American model facilities is the use of amplifying channels with large (~ 200 mm) aperture. This has made it possible to achieve even in the two-channel "Argus" facility high values of the laser-pulse power, and to develop the high-power "Shiva" facility which has only 20 parallel amplification channels.[9] Homogeneity of the illumination of a target irradiated from both sides was achieved by using beams with appreciable convergence solid angles at the target. The use of amplification elements with relatively small (45 mm diameter) aperture required, to achieve high laser-pulse energies, the use, even in the first generation of the Kal'mar of the USSR Physics Institute, of an appreciable number (nine) amplification channels connected in a series-parallel sequence.[12] Uniform irradiation was achieved by arranging the nine rays, which converged at small solid angles on the target, in a nearly spherical geometry. Further increase of the laser energy in the "Sokol" and "Del'fin" facilities is via an ever increasing number of amplification channels. A characteristic feature in this case is the merging of the laser rays into beams in the irradiation system. In the "Sokol" facility, rays from 24 amplification channels are pairwise connected into twelve beams arranged in a spherical geometry (the "Del'fin" facility of the USSR Physics Institute has twelve beams, each containing 18 rays[14]).

1. DRIVING LASER AND PRELIMINARY AMPLIFICATION STAGES

The optical system of the "Sokol" facility is illustrated in Fig. 1. The initial light pulse, in contrast to the "Kal'mar"
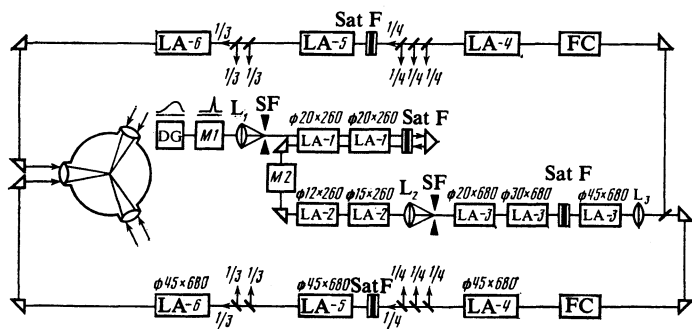
FIG. 1. Optical diagram of the "Sokol" facility: DG—driving laser; M1—optical shutter; L—lenses, SF—spatial filter; SatF—saturable filter; FC—Faraday cell, LA-1—first stage amplifier.

facility,[12,13] is shaped in a single-pulse driving laser with rapid-action Pockels cells using KDP crystals rather than Kerr cells. Optical shutters based on these crystals have a high operating speed, and are also capable of operating in high-intensity laser beams. The use of Kerr cells is limited by the low thresholds of the self-focusing and of the Raman scattering of nitrobenzene.[15] The high optical quality of the KDP and DKDP single crystals used in the optical shutters of the "Sokol" facility makes it possible to use these shutters to modulate the laser beams with divergence $\approx 3 \times 10^{-4}$ rad.

The driving generator of the "Sokol" facility is a neodymiun-glass Q-switched laser. The Q-switch is a Pockels cell using DKDP crystal of 10 mm diameter and 20 mm length. The transverse modes of the laser cavity are selected with the aid of a 3 mm diameter diaphragm placed in the cavity. The radiation pulses from the driving generator of the "Sokol" facility have parameters typical of the nominal operating regime, namely peak power $P = 7$ MW and beam divergence (at the $1/e$ level) $2\alpha \approx 5 \times 10^{-4}$ rad.

The high-speed optical shutters that separate a nanosecond pulse from the radiation of the driving generator are made up of KDP crystals of 10 mm diameter and 20 mm length, with strip electrodes of width $h = 3$ mm. The geometry, as shown in Refs. 16 and 17, is optimal from the point of view of simultaneously satisfying the condition that the field be homogeneous over the crystal cross section and that the optical shutter reach a maximum contrast. The polarizing devices for the optical shutters were Glan prisms of Iceland spar of "Extra" grad. As a result the individual value of the contrast (the ratio of the transmissions in the open and closed states) of each optical shutter M1 and M2 was not worse than 7×10^3. The sufficiently high optical strength of the KDP crystals made it possible to use these shutters in light fluxes with intensity up to one GW/cm².

The Pockels cells of the optical shutters M1 and M2 are controlled from a single nitrogen discharge gap ignited by a laser. This ensures reliable synchronization of the instant of operation of the shutter M1 with the emission of the driving laser, and automatically ensures mutual synchronization of the shutters M1 and M2.

To perform target-irradiation experiments the system for shaping the nanosecond light pulses was adjusted to produce pulses of minimum duration (determined by the operating speed ~ 0.7 nsec of the optical shutters). The time variation of the intensity of the laser pulse at the output of the shaping system was determined with an image converter operating in the slit scanning regime. To calibrate the scanning, the pulse was multiplied and the pulses with known repetition period were applied to the image-converter slit. Figure 2 shows the result of photometry of the image-converter pattern obtained with such a procedure. The laser-pulse duration obtained as a result of these measurements, at half-maximum level, was ~ 0.7 nsec.

Linear amplification stages are used for preamplification of the nanosecond light pulse. A spatial filter (focal length of the lens $f_1 = 1.8$ m, diaphragm diameter $d_1 = 1.0$ mm) was placed at the input to the first stage and improved the spatial-angular characteristics of the radiation past the optical shutter M1, producing a diverging beam $(2\theta_1 = 1.7 \times 10^{-3}$ rad). The first stage is constructed in the form of a two-pass amplifier with active elements made of GLS-1 glass, of 20 mm diameter and 260 mm length. In the first amplification stage the laser-pulse power increases from 3 to 150 MW. To prevent self-excitation in the first stage, a saturating filter (dye No. 3955 in nitrobenzene) with initial transmission $T_0 \approx 0.05$ is used.

The first and second amplification stages are separated by a contrasting optical shutter. The second stage consists of two amplifiers with active elements of GLS-1, with diameters 12 and 15 mm, and with length (both) 260 mm. In this stage, the laser-pulse power is raised to ≈ 1 GW. The second and third stages are separated by a spatial filter (effective focal length of the objective is $f_2 \approx 1.3$ m, the diaphragm diameter is $d_2 = 0.75$ mm). The output lens of the spatial filter is located past the final amplifier of the third stage (see Fig. 1) and has a focal length $f_3 \approx 5.2$ m. The third stage consists of
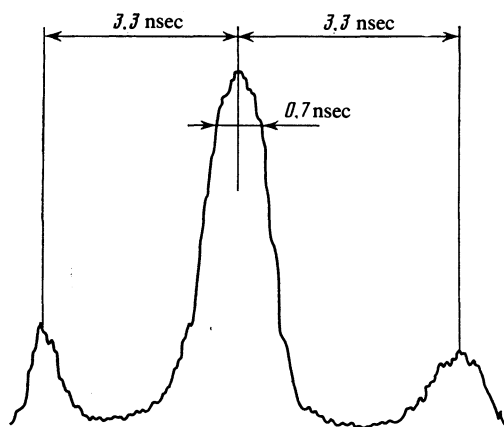

FIG. 2. Density pattern of laser pulse at the output of optical shutter M2; the pulse was multiplied by a system of mirrors to calibrate the image-converter sweep.

three amplifier with active elements of GLS-1 glass, with diameters 20, 30 and 45 mm respectively, and each 680 mm. In the target irradiation experiments, the laser pulse power did not rise above 25 GW.

2. POWER AMPLIFICATION STAGES

Further increase in the energy of the laser pulse in the power stages, just as in the "Kal'mar" and "Del'fin" facilitis,[12-14] was effected by increasing the number of amplification channels while keeping constant (45 mm diameter) the aperture of each channel. The power stages of the "Sokol" facilities were in accord with a series-parallel scheme: 1(1)–2(2)–4(8)–3(24). The first numbers correspond to the division coefficient and the numbers in the parenthesis to the number of amplification channels in the stage. In all the amplification channels of the high-power stages we used amplifiers with elements of GLS-1 neodymium glass, 45 mm in diameter and 680 mm long.

The light beam was split with amplitude dividers. The divider was a plane-parallel glass plate, one side of which was coated with a dielectric mirror resistant to light, and the other with a nonreflecting coating.

To protect against the laser radiation reflected from the target, Faraday cells were placed at the outputs of the preamplification stages. Self-excitation of the amplification channel in the power stages was prevented by saturable filters with initial transmission $T_0 \approx 0.05$.

In the experiments on target irradiation with the "Sokol" facility, the radiation intensity at the output of the power stages did not exceed as a rule ≈ 1 GW/cm^2. Under these conditions, the main parameters of the laser pulse at the output of the power stages were the following: laser pulse energy $E_L \approx 300$ J; peak power $P \approx 0.4$ TW; radiation divergence (at the $1/e$ level) $2\alpha \approx 3 \times 10^{-4}$ rad; energy contrast $\sim 10^6$.

The experiments have shown that with increasing intensity level in the amplifier power stages the quality of the laser beam deteriorated and the wave form of the laser pulse was strongly distorted (Fig. 5). The reason was that, owing to the large length of the amplifier active medium past the last spatial filter, an appreciable accumulation of perturbations

FIG. 3. Distortion of the shape of the laser pulse as a result of small-scale self-focusing in the power stages of amplification of $I_{out} \sim 2$ GW/cm^2.

of the laser radiation wavefront takes place, as a result of the small-scale self-focusing, as soon as the power-stage output intensities reach $I_{out} \gtrsim 1$ GW/cm^2.

It is significant in this connection that the power of the laser pulse at the output of the preamplification stages could be raised to $P \approx 35$ GW, corresponding to laser-radiation intensities 2 GW/cm^2; the beam divergence did not exceed in this case $2\alpha \approx 3 \times 10^{-4}$ rad, and no dips were observed in the time dependence of the laser-pulse intensity.

3. TARGET IRRADIATION SYSTEM

The chamber of the "Sokol" target is similar to that of the "Del'fin"[14] and makes possible spherical irradiation of the targets. The chamber has 12 two-lens objectives corrected for chromatic and spherical aberration. The objectives have a focal length $F = 300$ mm, an aperture $d = 110$ mm, and a resolution $\Delta \lesssim 90 \mu$m. Two laser rays are joined together in each lens. The lenses are arranged on the spherical surface of the chamber to form a cube in such a way that light rays passing through the lenses on one face and the center of the chamber do not land in lenses located on the opposite face. The angular coordinates of the lenses are given in Table I. Compared with the chamber of the "Del'fin" facility,[14] the lens coordinates were modified to obtain a more uniform arrangement of the lenses over the sphere.

The laser rays converged in the chamber on the target located at the center of the chamber, with the optical paths adjusted to ensure simultaneous arrival of the laser pulses from all the amplification channels. The arrival times of the target-irradiating pulses were synchronized with accuracy not worse than 0.05 nsec. Preliminary tuning of the optical channels of the "Sokol" facility was with and He-Ne laser, and the final tuning with a infrared yttrium-aluminum-garnet "Congo-1" laser. The measurements have shown that the procedure used to tune the "Sokol" facility ensures an accuracy of directing the beams on the target not worse than 10 μm.

One of the important requirements imposed on the irradiation system by the peculiarities of the experiments on compression of spherical targets is a high,[18-20] $\sim 10\%$, homogeneity of the illumination on the target.

Calculations performed in Ref. 21 for a 12-beam (see Table I) geometry of irradiation have shown that, assuming a Gaussian distribution of the intensity in the light beam and in the plane wavefront in the target region, the illumination uniformity will be $\gamma \approx 10$–20% at $\rho_e = R_t$ (here ρ_e is the dimension of the light beam at the $1/e$ level, and R_t is the target radius). The uniformity of the illumination was defined as $\gamma = \Delta\Phi / \Phi_{av}$ ($\Delta\Phi$ is the difference between the maximum and minimum illuminations, and Φ_{av} is the average illumination). The fraction of the radiation incident on the target under these conditions is quite high, $\eta \approx 50$–70%. Calculations have shown that at the laser-pulse parameters typical of the "Sokol" facility the maximum radius R_{cr} of the plasma region with critical density, for irradiated shell targets with $R_t \approx 50$–60 μm, will have a value $R_{cr} \approx 70$–80 μm. The condition $\rho_e \approx R_{cr}$ was satisfied by adjusting the focal plane of the objectives behind the target in such a way that

TABLE I.

Lens No.	1	2	3	4	5	6	7	8	9	10	11	12
θ, deg.	23	23	106	74	106	74	106	74	106	74	157	157
φ, deg.	0	180	16	74	106	164	196	254	286	344	90	270

the laser-beam diameter on the target (at the $1/e$ intensity level) was $150\,\mu$m.

The maximum radiation flux density on the target $q = P_c/4\pi\rho_e^2$ (P_c is the power of the laser radiation in the chamber) reached in the experiments, with the "Sokol" facility with the objectives so adjusted, was $q \approx 3\cdot10^{14}$ W/cm^2.

4. DETERMINATION OF THE LASER ENERGY ABSORBED BY THE TARGET

Measurement of the absorbed energy E_{abs} in one of the important aspects of research into interaction of laser radiation with a plasma and of the analysis of the gas dynamic processes of the expansion, compression, and heating of the thermonuclear fuel of the laser targets. The absorbed laser energy E_{abs} is released in the form of x rays E_x from the dense and hot parts of the plasma, thermal energy E_{th}, and kinetic energy E_{kin} of the gas dynamic motion of the target material:

$$E_{abs} = E_x + E_{th} + E_{kin}.$$

The interaction of the radiation with the plasma is characterized by the energy E_{abs}; the compression is determined by the sum of the energies $E_{th} + E_{kin}$, and the x-ray energy E_x constitutes the losses. The determination of the total gasdynamic energy $E_g = E_{th} + E_{kin}$ is presently carried out by diagnostic methods based either on the analysis of the ions of the expanding plasma, registered with the aid of ion collectors,[22-24] or by registering the $(R-t)$ parameters of the shock
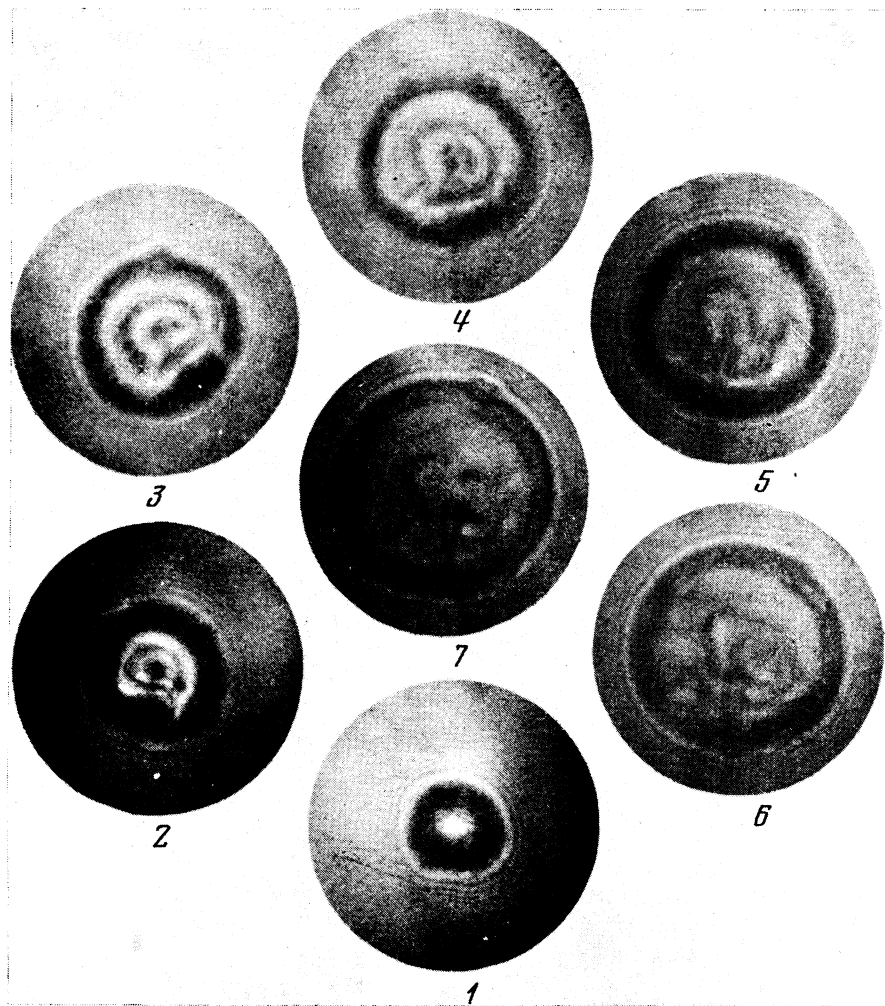

FIG. 4. Shadow photographs of the propagation of a shock wave in the atmosphere of a residual gas in the target chamber. Air pressure $P_0 = 3.45$ Torr; laser-pulse energy in the target region $E_0 = 81$ J; frames 1–7 were exposed at the instants of time 10.2, 42, 74, 107, 139, 169, and 200 nsec, respectively.

wave (SW) propagating in the atmosphere of the gas surrounding the target.[25-27]

The measurement of E_g in experiments on spherical irradiation of targets in the "Sokol" laser facility was carried out by the "shock wave" method. The $(R-t)$ parameters of the SW were recorded by multiframe shadow photography of the propagation of the shock wave in the atmosphere of the gas surrounding the target (air was used in the present experiment).[12,24] Typical results of the shadow photography of the shock wave are shown in Fig. 4.

The technique of reducing the experimental $(R-t)$ parameters of the SW for the purpose of determining the energy E_g can be based on Sedov's[28] self-similar law (1), as was done, e.g., in Refs. 12, 26, and 27:

$$R(t) = \xi_0 (E_g/\rho_0)^{1/s} t^{2/s}, \tag{1}$$

where ρ_0 is the density of the surrounding gas; t is the time; ξ_0 is a dimensional factor ($\xi_0 = 1.12$ for $\gamma = 5/3$). It must be borne in mind that laser heating is subject to a number of irregularities[26,29] that lead to deviation of the experimental $(R-t)$ parameters of the SW from the law (1); this was observed both in Refs. 12 and 26 and in the present work. The most substantial are the following: First, the high electronic thermal conductivity of the laser plasma produces a thermal wave that propagates rapidly in the gas surrounding the target. The shock wave propagates therefore in a perturbed gas and this leads to a deviation of the $(R-t)$ parameters of the SW from the self-similar law (1). Second, the real equation of state of the surrounding gas differs from that of an ideal gas. Third, deviation of the experimental $(R-t)$ parameters of the SW from the self-similar law (1), can also be due to radiation energy losses of energy from the gas subtended by shock-wave front. Correct allowance for all the foregoing factors makes it necessary to reduce the experimental $(R-t)$ parameters of the SW, when determining the energy E_g, by using gas dynamic calculations of the expansion of the target and of the motion of the shock wave through the gas surrounding the target.

The laser energy absorbed by the target was determined by gas dynamic calculations using the "Zarya" program. We used interpolated equations of state, and took into account the electronic thermal conductivity, the ion viscosity, and the losses to radiation. For aid we used an interpolation equation of state and Planck mean free path, which make it possible to interpolate the results of Ref. 30, with ≈ 10–15% accuracy, in the region

$$3 \cdot 10^{-6} \leq \rho \, [\text{g/cm}^3] \leq 3 \cdot 10^{-4}, \quad 2 \leq T \, [\text{eV}] \leq 100$$

(T is the temperature on the SW front).

Experimental data on the SW for one of the experiments and the results of calculations of $E_{abs} = 9$ J are shown in Fig. 5. In the region with $T \geq 2$ eV, the calculated $(R-t)$ diagram passes through the experimental points. The deviation in the case of the first frame ($t_1 = 10.2$ nsec) can be attributed to the fact that at small SW radii the details of the energy transfer from the target to the residual gas come into play. The discrepancy between the calculated $(R-t)$ diagram of the SW and the experimental points for the last two frames ($t_6 = 169$ nsec; $t_7 = 200$ nsec) can be due both to the inaccuracy of the
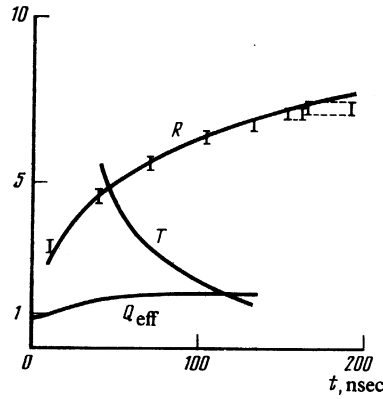

FIG. 5. Experimental and calculated $(R-t)$ shock-wave diagrams; the temperature on the shock-wave front (T) is in electron volts; the loss to radiation (Q_{eff}) is in J; R is in millimeters.

extrapolation of the equation of state of the air of $T < 2$ eV and to the fact that at shock-wave velocities $D \sim 10$ km/sec an essential role can be played by the disequilibrium of the ionization. The characteristic ionization time at this shock-velocity and at an air pressure $P_0 \approx 3.4$ Torr is 10–30 nsec if the results of Ref. 30 are extrapolated into the region of high energies. Introduction, on the other hand, of only the correction due to the disequilibrium of the ionization leads to a better agreement between the calculated and the experimental data for the last two points (See Fig. 5).

The procedure of determining E_g with the aid of gasdynamic calculations is quite laborious and does not make it possible to obtain effectively the absorbed energy immediately after the experiment. Calculations were therefore performed, using the "Zarya" program, in a three-temperature approximation, for the purpose of obtaining the interpolation dependence of the radius of the SW front on the time for different values of the energy and pressure of the air surrounding the target. These calculations have shown that the dependence of the SW radius on the time can be represented by the expression

$$R_{SW}[\text{mm}] = 1.126 \, (E_g/P_0)^{1/4} t^{1/4} \, [\text{nsec}], \tag{2}$$

where P_0 [Torr] is the pressure of the air surrounding the target. In the region $5 \leq E_g$ [J] ≤ 50 and $2 \leq P_0$ [Torr] ≤ 5, Eq. (2) interpolates the calculated SW front radius accurate to $\approx 1\%$.

The obtained expression (2) differs from Sedov self-similar law (1). This is due, as indicated above, to allowance for the radiation losses and to the difference between the interpolation equation of state of the air from that of an ideal gas. The restrictions on the applicability of expression (2) at high SW radii and long times is due to the fact that the interpolation equation of state used for air in the present paper ensures the required accuracy only in the region $T > 2$eV. This condition leads to the requirement

$$R_{SW}[\text{mm}] = 4.73 \, (E_g/P_0)^{1/4} \quad \text{or} \quad D > 22 \text{ km/sec}, \tag{3}$$

where D is the shock-wave speed.

A restriction at small SW radii is imposed by the requirement that the mass of the air included in the shock-wave front exceed the target mass by ≈ 3–5 times.

TABLE II.

Frame No.	1	2	3	4	5	6	7
t_i, nsec	10.2±0.8	42±0.8	74±0.8	107±0.8	139±0.8	169±0.8	200±0.8
R_{SW}, mm	3.6±0.2	5.3±0.2	6.3±0.2	7.3±0.2	7.8±0.2	8.1±0.2	8.4±0.2
E_g, J	16±4	11.6±1.8	10.9±1.5	12±1.3	11±1.1	9.9±1	9.1±0.9
E_g^*, J	31.8	13	9.9	9.9	8.2	6.7	5.7

Note. t_i are the instants of time of exposure of the SW frames; R_{SW} is the shock-wave radius; the total gas dynamic energies determined from (2) and (1) are E_g and E_g^*.

Table II gives the $(R-t)$ parameters in air, measured in one of the experiments (see Fig. 4) with the "Sokol" facility. The table lists also the values of the energy E_g determined from Eqs. (1) and (2). The last two values of E_g, calculated from Eq. (2), should be disregarded, since the condition (3) is not satisfied for them. The total relative error in the determination of the energy is 20–25% and is due mainly to the error in the determination of the position of the shock-wave front. The most probable value determined from the first five frames is $E_g = 11.5 \pm 2.3$ J. Since the x-ray energy is shown by calculation to be $E_x \approx (0.1–0.2) E_{abs}$, the laser energy absorbed by the target is $E_{abs} = 13.6 \pm 2.3$ J. As seen from Table II, the self-similar relation (1) does not fit the experimental $(R-t)$ diagram of the SW and therefore cannot be used to determine the total gas dynamic energy E_g.

CONCLUSION

The development of the "Sokol" 24-channel laser facility has made it possible to continue the experiments, initiated in 1976 with the "Kal'mar" facility, on irradiation of gas-filled glass microspheres by nanosceond pulses at higher flux densities at the target. The experiments were carried out in the range $q \approx 10^{13}–3 \times 10^{14}$ W/cm^2.

Further increase in the light-flux density at the target by increasing the laser-pulse power was hindered by the development of small-scale self-focusing of the beam in the power stages of the amplifiers. It appears that this effect is a serious obstacle to obtaining appreciable laser-beam intensities in the amplificlation channels of facilities based on the series-parallel scheme. A characteristic feature of this scheme is that the intensities of the laser beams at the outputs of all the power stages are approximately equal, making it energywise more effective compared with the parallel scheme.[13] But such an amplification regime, as shown by the analysis[31-33] of the evolution of small-scale self focusing, is less convenient compared with the regime obtained in the parallel scheme of the power stages, in which the maximum intensity is reached at the output of the amplification channels. However, a consistent use of measures for the suppression of the development of small-scale self-focusing,[33] particularly the use of spatial filters to separate the amplification-channel stages, promises to yield high output values of the intensity, $\approx 3–5$ GW/cm^2 also in facilities with series-parallel connection of the amplifier power stages.

[1]N. G. Basov and O. N. Krokhin, Zh. Eksp. Teor. Fiz. 46, 171 (1964) [Sov. Phys. JETP 19, 123 (1964)].
[2]N. G. Basov and O. N. Krokhin, Vestnik AN SSSR 6, 55 (1970).

[3]K. Brueckner and S. Jorna, Rev. Mod. Phys. 46, 325 (1973).
[4]Yu. V. Afanas'ev, N. G. Basov, P. P. Volosevich, et al., Pis'ma Zh. Eksp. Teor. Fiz. 21, 150 (1975) [JETP Lett. 21, 68 (1975)].
[5]R. J. Mason and R. Z. Morse, Phys. Fluids 18, 814 (1975).
[6]R. J. Mason and R. Z. Morse, Nuclear Fusion 15, 935 (1975).
[7]L. P. Feoktistov, E. N. Avrorin, L. F. Varganova, A. D. Gadzhiev, V. A. Lykov, V. Z. Nechaĭ, and L. I. Shbarshov, Kvant. Elektron. (Moscow) 5, 349 (1978) [Sov. J. Quantum Electron. 8, 201 (1978)].
[8]T. M. Henderson and R. R. Johnson, Appl. Phys. Lett. 31, 18 (1977).
[9]Solid State Program, in: Laser Program Ann. Report, 1976, LLL Report UCRL-50021076, June 1977.
[10]E. K. Storm, H. G. Ahlstrom, M. J. Boyle, et al., Phys. Rev. Lett. 40, 1570 (1978).
[11]V. W. Slyvinsky, H. G. Ahlstrom, J. H. Nuckolls, et al., J. Appl. Phys. 49, 1106 (1978).
[12]N. G. Basov, O. N. Krokhin, G. V. Sklizkov, S. I. Fedotov, and A. S. Shikanov, Zh. Eksp. Teor. Fiz. 62, 203 (1972) [Sov. Phys. JETP 35, 109 (1972)].
[13]N. G. Basov, O. N. Krokhin, G. V. Sklizkov, and S. I. Fedotov, Trudy FIAN, 76, 146 (1974).
[14]N. G. Basov, N. E. Bykovskiĭ, A. E. Danilov, et al. Trudy FIAN 103, 3 (1978).
[15]Spravochnyk po lazeram (Laser Handbook), A. M. Prokhorov, ed., Vol. 2, Sov. Radio, 1978, p. 271.
[16]M. G. Vitkov, Opt. Spektrosk. 24, 786 (1968).
[17]L. L. Steinmetz, T. W. Pouliot, and B. C. Johnson, Appl. Opt. 71, 1468 (1973).
[18]Proc. 5th Internat. Conf. on Plasma Physics and Contr. Nucl. Fusion, Tokyo, 11–15 Nov. 1974, Vol. II. Yu. V. Afanas'ev, N. G. Basov, P. P. Volosevich, et al., p. 559 J. Nuckolls, J. Lindl, W. Mead, et al., p. 535; G. Fraley, W. Gala, D. B. Henderson, et al., p. 543.
[19]A. A. Bunatyan, V. E. Nuevazhaev, L. P. Strotseva, and V. A. Frolov, Preprint IPM-71, 1975.
[20]N. N. Bokov, A. A. Bunatyan, V. A. Lykov, V. E. Neuvazhaev, L. P. Strotseva, and V. D. Frolov, Pis'ma Zh. Eksp. Teor. Fiz. 26, 630 (1977) [JETP Lett. 26, 478 (1977)].
[21]V. V. Volenko and V. B. Kryuchenkov, Kvant. Elektron. (Moscow) 6, 1343 (1979) [Sov. J. Quantum Electron. 9, 789 (1979)].
[22]J. Soures, L. M. Goldman, and M. Lubin, Nuclear Fusion 13, 829 (1973).
[23]R. R. Goforth, Rev. Sci. Instr. 47, 548 (1976).
[24]P. M. Campbell, R. R. Johnson, F. J. Mayer, et al., Phys. Rev. Lett. 39, 274 (1977).
[25]N. G. Basov, V. A. Gribkov, O. N. Krokhin, and G. V. Sklizkov, Zh. Eksp. Teor. Fiz. 54, 1073 (1968) [Sov. Phys. JETP 27, 575 (1968)].
[26]N. G. Basov, E. G. Gamaliĭ, O. N. Krokhin, Yu. A. Mikaĭlov, G. V. Sklizkov, and S. I. Fedotov, FIAN Preprint 15, 1974.
[27]V. G. Gribkov, V. Ya. Nikulin, O. G. Semenov, and G. V. Sklizkov, Fiz. Plazmy 4, 1056 (1978) [Sov. J. Plasma Phys. 4, 589 (1978)].
[28]Ya. B. Zwl'dovich and Yu. P. Raizer, Physics of Shock Waves and High-Temperature Hydrodynamic Phenomena, Academic, 1966–7.
[29]V. Ya. Gol'din and B. N. Chetverushkin, Zh. Eksp. Teor. Fiz. 68, 1768 (1975) [Sov. Phys. JETP 41, 885 (1975)].
[30]N. Kuznetsov, Termodinamicheskie funktsii i udarnye adiabaty vozdkha pri vysokikh temperaturakh (Thermodynamic Functions and Shock Adiabats of Air at High Temperatures), Mashinostroenie, 1965.
[31]Small-Scale Instability Growth, in: Laser Program Annual Report, 1974, LLL Report UCRL-50021-74, March 1975, p. 139.
[32]Theory of Irregularity Growth of Laser Beams, in: Laser Program Annual Report, 1975, LLL Report UCRL-50021-75, March 1976, p. 339.
[33]N. B. Baranov, N. E. Brykovskiĭ, Yu. V. Senatskiĭ, and S. V. Chekalin, Trudy FIAN 103, 84 (1978).

Translated by J. G. Adashko